1 **Long-term pig manure application increases SOC through aggregate protection and Fe-C**

2 **associations in a subtropical Red soil (Udic Ferralsols)**

3 Hui Rong[a], Zhangliu Du[b], Weida Gao[a], Lixiao Ma[c], Xinhua Peng[d], Yuji Jiang[e], Demin Yan[f], Hu Zhou[a,]

4 [a] *Key Laboratory of Arable Land Conservation (North China), Ministry of Agriculture, College of Land Science and*

5 *Technology, China Agricultural University, Beijing 100093, China*

6 [b] *College of Resources and Environmental Sciences, China Agricultural University, Beijing 100193, China*

7 [c] *State Key Laboratory of Vegetation and Environmental Change, Institute of Botany, Chinses Academy of Sciences,*

8 *Beijing 100093, China.*

9 [d] *Institute of Agricultural Resources and Regional Planning, Chinese Academy of Agricultural Sciences, Beijing*

10 *100081, China*

11 [e] *College of Resources and Environment, Fijian Agriculture and Forest University, Fuzhou, 350002, China.*

12 [f] *College of Criminal Science and Technology, Nanjing Police College, Nanjing 210023, China.*

13 **Correspondence**: Hu Zhou (zhouhu@cau.edu.cn)

14 **Abstract**

15   Manure is known to improve soil organic carbon (SOC) in Fe-rich red soils, but the underlying

16 stabilization mechanisms remain poorly understood. A long-term field experiment was conducted

17 with four treatments: no amendment (Control), low manure (LM, 150 kg N ha^{-1} yr^{-1}), high manure

18 (HM, 600 kg N ha^{-1} yr^{-1}), and high manure with lime (HML, 600 kg N ha^{-1} yr^{-1} plus 3000 kg Ca

19 (OH)$_2$ ha^{-1} (3yr)$^{-1}$). The quantity and quality of SOC were characterized by physical fractionation,

20 ^{13}C NMR spectroscopy and thermogravimetry (TG) analysis from 0-20 cm depth. 18-yr manure

21 application increased total SOC by 65.1%-126.7%, with the increase primarily occurring in the

22 particulate organic matter (POM) fraction. Specifically, POM C increased substantially by 208%-

23 592%, compared to a 32.0%-66.8% increase in MAOM C. POM C was stabilized through the

24 process of hierarchical aggregation. Fresh manure inputs acted as binding nuclei, leading to an

25 increase in macroaggregates (>0.25 mm) concurrently with a reduction in microaggregates (0.05–

26 0.25 mm), physically isolating labile C from microbial decomposition. Concurrently, manure

27 amendments triggered Fe-mediated chemical stabilization. The elevated pH (4.8 to 5.4-7.1) in the

28 manure treatments enhanced non-crystalline Fe oxide (Fe$_o$) content by 25.4%, which positively

29 correlated with MAOM C (R^2=0.56, P<0.05). Despite chemical composition shift toward

30 aliphaticity and reduced aromaticity, thermally stable organic matters increased by 8%–12%,

31 revealing the critical role of Fe_o in offsetting inherent molecular lability when aggregate protection

32 was removed by destruction prior to TG analysis. Overall, this study proposes a dual SOC

33 stabilization framework via physical and chemical Fe-carbon associations in a subtropical red soil.

34 **Keywords**: Particulate organic matter; Mineral-associated organic matter; Nuclear magnetic

35 resonance; Thermogravimetry analysis

36

1. Introduction

38 Soil organic carbon (SOC), the largest carbon reservoir in the terrestrial ecosystems, plays critical

39 roles in climate mitigation and soil multifunctionality (Amelung et al., 2020; Lal, 2004). Red soils

40 (Udic Ferralsols, according to Chinese Soil Taxonomy) have low SOC content due to intense

41 weathering and rapid mineralization in tropical and subtropical South China (Yan et al., 2013; Zhang

42 et al., 2013). While manure has been widely used to enhance SOC in these soils (Bai et al., 2023;

43 Nichitha et al., 2023; Zhang et al., 2023), the underlying mechanisms governing its stabilization

44 remain elusive. Currently, the discrepancies existed regarding the manure-induced SOC accrual

45 through chemical recalcitrance, physical protection (by aggregation processes), or organo-mineral

46 interactions—given the Fe-enrich red soils and their pH-dependent reactivity (Kleber et al., 2021;

47 Six et al., 2002; Song et al., 2022). Considering the red soils covering 22% of China's cropland and

48 low inherent SOC levels, it is essential to unveil Fe-C interactions that regulate SOC stabilization

49 through organic amendments.

50 Existing studies showed some conflicting evidences on SOC stabilization pathways. For instance,

51 Mustafa et al. (2021) reported increased aromatic C (chemically recalcitrant) with manure

52 application, whereas Yan et al. (2013) observed preferential accumulation of labile O-alkyl C. This

53 paradox highlighted uncertainties on how manure inputs altered SOC composition. It is reported

54 that Fe oxides contributed to SOC stabilization in red soils (Zhang et al., 2013). These reactive Fe

55 phases can form stable covalent bonds between their surface hydroxyls and organic functional

56 groups, protecting SOC from microbial decomposition (Ruiz et al., 2024). In comparison with

57 crystalline Fe oxides (Fe_d), non-crystalline Fe oxides (Fe_o) exhibit organic matter adsorption

58 capacity primarily attributed to their larger specific surface area (Zhang et al., 2013). Previous

59 studies have demonstrated that long-term application of organic fertilizers—including manure,

60 compost, and straw—significantly increased non-crystalline iron oxides (Fe_o) in agricultural soils

61 (Chen et al., 2022; Huang et al., 2018; Wang et al., 2019). These studies further revealed that redox

62 cycling promoted the reductive dissolution of crystalline iron (Fe_d), followed by its reprecipitation

63 as amorphous Fe_o during oxidative periods. On the other hand, soil pH was identified as a key factor

64 dynamically influencing the Fe_d/Fe_o ratio (Liu et al., 2020; Wang et al., 2023). Although organic

65 amendments are known to elevate pH in acidic red soils, the specific effect of soil pH modulating

66 the formation and stabilization of Fe_o remains unclear. Additionally, previous studies widely isolated

67 chemical recalcitrance, aggregation protection, or organo-mineral interactions separately, largely

68 neglecting the integrative assessments including these pathways. To address this knowledge gap, an

69 integrative approach combining physical fractionation, molecular characterization, and thermal

70 stability analysis is essential for elucidating the coupled effects of manure on SOC quantity and

71 quality.

72   Physically separating soil organic matter (SOM) into mineral-associated organic matter (MAOM)

73 and particulate organic matter (POM) fractions could help to predict SOC dynamics, and clarify

74 SOC stabilization mechanisms. The POM associated SOC (defined as POM C) physically protected

75 in the macroaggregates, while MAOM associated SOC (defined as MAOM C) chemically protected

76 via organo-mineral bonding (Chenu et al., 2019; Lavallee et al., 2019; Poeplau et al., 2018).

77 Although physical fractionation could effectively isolate operationally defined these SOC pools

78 (Poeplau et al., 2018), it failed to reveal the chemical heterogeneity of SOC (Cotrufo et al., 2019;

79 Lavallee et al., 2019). Thus, solid-state ^{13}C NMR spectroscopy could address this gap by quantifying

80 SOC functional groups (e.g. alkyl, O-alkyl, aromatic C), after completely disrupting organo-mineral

81 interaction by HF pretreatment (Kögel-Knabner, 1997). Additionally, the thermogravimetry (TG)

82 could rapidly assess the thermal stability of SOC without requiring pretreatment (Gao et al., 2015).

83 On the other hand, some advanced techniques such as nano-scale secondary ion mass spectrometry

84 (Nano-SIMS) and high-resolution mass spectrometry could identify the spatial visualization of

85 organo-mineral associations and molecular characterization, these approaches heavily required

86 complex instrumentation and are not cost-effective for the comparative analysis of multiple samples.

87 Therefore, combined NMR with TG approaches to efficiently evaluate the chemical composition

88   and thermal stability of SOC in response to manure management.

89   The specific objectives of this study were: 1) to evaluate the changes of Fe oxides and its effect

90   on MAOM formation; 2) to explore how soil aggregation affected POM formation; 3) to evaluate

91   the effect of manure application on SOC composition and stability. We hypothesized that: 1) Manure

92   application could enhance MAOM C formation by increasing non-crystalline Fe oxides (Fe_o),

93   induced by elevated pH; 2) Manure application would strengthen the physical protection due to the

94   improved soil aggregation, which triggered labile SOC protection; 3) The application of pig manure

95   would boost the recalcitrance of SOC, thus the thermal stability.

96

97   **2. Materials and methods**

98   *2.1. Site description and experimental design*

99   The long-term field experiment is located at Yingtan National Agroecosystem Field Experiment

100   Station of the Chinese Academy of Sciences (28°15′20″N, 116°55′30″E) in Jiangxi Province, China.

101   The site has a typically subtropical humid monsoon climate with a mean annual temperature of 17.6℃

102   and precipitation of 1795 mm (Jiang et al., 2018). The soil is derived from Quaternary red clay, and

103   is classified as Udic Ferralsols according to Chinese Soil Taxonomy. The soil contains 36.3% clay,

104   45.2% silt and 21.2% sand.

105   The field experiment was initiated in April, 2002. The soils used in this experiment were

106   transported from adjacent forestland and repacked (to a depth of 2 m) for all the plots. This design

107   ensures a uniform initial soil condition and eliminates the influence of prior land use history. Four

108   treatments were compared: (1) no manure amendment (Control), (2) low pig manure with 150 kg N

109   ha^{-1} a^{-1} (LM), (3) high pig manure with 600 kg N ha^{-1} a^{-1} (HM), and (4) high pig manure with 600

110   kg N ha^{-1} a^{-1} and lime applied at 3000 kg Ca $(OH)_2$ ha^{-1} $(3a)^{-1}$ (HML). The four treatments received

111   solely pig manure as the nitrogen source, with no synthetic fertilizers applied. The pig manure,

112   collected from nearby pig farms, contained an average total carbon of 386.5 g kg^{-1}, total nitrogen of

113   36.2 g kg^{-1} and total phosphorus of 21.6 g kg^{-1} on a dry matter basis. The annual amount of pig

114   manure applied to each treatment was calculated based on its nitrogen content. Since all

115   aboveground residues (stalks and leaves) and manually recoverable roots were completely removed

116   from the field after harvest, the total carbon inputs to the soil were derived mainly from pig manure**.**

117   This resulted in average annual carbon inputs of around 1.6 and 6.4 Mg C ha^{-1} for the LM and HM

118   treatments, respectively (see Supplementary Material for calculation details). The field experiment

119   was set up following a completely randomized design, with each treatment has three replicate plots.

120   The field was planted with corn (*Zea mays L.*) monoculture annually from April to July. The pig

121   manure was applied annually each April onto the soil surface (0-10 cm depth) and subsequently

122   incorporated into the topsoil through plowing and harrowing. All the management measures,

123   including sowing, harvesting and weeding, were manually operated.

124   *2.2 Sampling*

125   Sampling was conducted in July 2019, after the harvest of corn. Triplicate topsoil samples (0-20

126   cm) were randomly collected with a shovel from each plot and composited together to form one

127   bulk sample. The soil samples were air-dried at room temperature and were gently crushed with a

128   rubber mallet to pass through an 8-mm sieve, preserving aggregates >8mm for further analysis.

129   Visible plant residues, roots and stones were removed (Soil Survey Staff, 2011). No visible manure

130   residues were observed.

131   *2.3 Soil properties measurements*

132   SOC and Total nitrogen (TN) were determined by an elemental analyzer (Vario MACRO,

133   Elementar, Germany). Soil pH was measured using a glass electrode (PHS-3D, SANXIN, China)

134   with soil: deionized water ratio of 1: 2.5. Crystalline (Fe_d) and non-crystalline Fe oxides (Fe_o) were

135   extracted by DCB (Dithionite-citrate-bicarbonate) and oxalate, respectively (Yan et al., 2013), and

136   then were determined by graphite furnace atomic absorption spectrometry (GFAAS) (PinAAcle

137   900T, PerkinElmer, America). Water stability of aggregates was tested using the fast-wetting method

138   following Le Bissonnais (1996). Aggregate stability was expressed as mean weight diameter

139   (MWD). Detailed experimental processes and calculation can be found in Zhou et al. (2019).

140   *2.4. Physical fractionation*

141   Soil was fractionated into MAOM (<53 μm) and POM (>53 μm) fraction following Cambardella

142   and Elliott (1992) and Cotrofu et al. (2019). Briefly, 10 g sieved samples (<2 mm) were dispersed

143   in dilute sodium hexametaphosphate (($NaPO3$)$_6$, 0.5%) at a soil: solution ratio of 1:4 by shaking for

144   18 h (25°C, 180 r min^{-1}). This procedure primarily disrupts macroaggregates (>250 μm), but

145   remaining that stable microaggregates (<53 μm). After dispersing, soil slurry was passed through a

53 μm sieve and rinsed several times with deionized water. The fraction passing through the sieve was collected as MAOM fraction, and that remaining on the sieve was collected as POM fraction. Both fractions were centrifuged and the solution was decanted, and then the remaining material was oven-dried to constant weights at 60°C. SOC concentration of each fraction was measured using the wet oxidation method. Dried mass proportions of each fraction (g fraction g^{-1} soil) were calculated as follows:

$$f_M = m_M / m_{bulk} \qquad (1)$$

$$f_P = m_p / m_{bulk} \qquad (2)$$

where f_M and f_P were the dried mass proportions of MAOM and POM fraction (g fraction g^{-1} bulk soil), respectively; m_M and m_P (g) were the dried masses of MAOM and POM fractions; m_{bulk} (g) was the dried mass of bulk soil.

SOC in the MAOM and POM fractions were called as MAOM C and POM C, respectively in this paper. MAOM C and POM C were calculated by multiplying the dried mass proportions of each fraction (g fraction g^{-1} soil) by the respective SOC concentrations (g C kg^{-1} fraction) as follows (Garten and Wullschleger, 2000; Lian et al., 2015):

$$MAOM\ C = f_M \times SOC_M \qquad (3)$$

$$POM\ C = f_P \times SOC_P \qquad (4)$$

where f_M and f_P were calculated by Equation (1) and Equation (2); SOC_M and SOC_P were the SOC concentrations in the MAOM and POM fraction (g C kg^{-1} fraction), respectively.

The contributions of MAOM C and POM C to total SOC (%) was calculated as:

$$Contribution\ of\ MAOM\ C\ (\%) = MAOM\ C\ /\ Total\ SOC \times 100\% \quad (5)$$

$$Contribution\ of\ POM\ C\ (\%) = POM\ C\ /\ Total\ SOC \times 100\% \quad (6)$$

where MAOM C and POM C were derived from Equations (3) and (4), respectively; total SOC was the content of SOC in the bulk soil.

2.5. SOC chemical composition and chemical stability

SOC chemical composition was analyzed with a solid-state cross-polarization magic angle spinning (CPMAS) ^{13}C nuclear magnetic resonance (NMR) spectroscopy. Prior to NMR analysis, <2 mm air-dried soils were pretreated with hydrofluoric acid (HF) to remove paramagnetic Fe^{3+} (iron oxides) following Gao et al. (2021). While HF pretreatment can dissolve short-range-order

175 minerals and potentially disrupt certain organo-mineral associations, it is an essential step to

176 improve the signal-to-noise ratio and spectral resolution required for the reliable quantification of

177 carbon functional groups. Firstly, 20 g soil was mixed with 100 mL 10% (w/w) HF solution in a

178 polyethylene bottle and then shaken for 0.5 h per day for three days. Afterwards, the supernatant

179 liquid was discarded and another 100 mL 10% HF solution was added again. The above procedures

180 were repeated for 15 times. The residue was rinsed 10 times with deionized water until the pH was

181 close to neutral. The remaining soil was freeze-dried and then ground in an agate mortar to pass

182 through a 100-mesh sieve (0.149 mm) for further analysis. This fine grinding ensured homogeneous

183 packing in the NMR rotor, minimizing signal heterogeneity (Simpson & Simpson, 2012).

184 Carbon functional groups were determined with the Bruker Ascend 500 MHz NMR spectrometer

185 (Bruker BioSpin, Rheinstetten, Germany). Dry powdered samples were placed in a 4-mm sample

186 rotor operating at a ^{13}C resonance frequency of 125.8 MHz. The NMR spectrometer run at a spinning

187 rate of 5kHz, and 10500 scans were collected for each sample. The spectra were collected over an

188 acquisition time of 12 ms and a recycle delay of 0.8 s. All obtained spectra were processed with

189 phase and baseline corrections. To allow for a direct comparison of the relative distribution of carbon

190 functional groups, the total spectral intensity of each spectrum was normalized to that of the Control

191 soil sample. The normalized spectra were then integrated across and we assigned the obtained

192 spectra to four different carbon functional groups, i.e., alkyl C (0-45 ppm), O-alkyl C (45-110 ppm),

193 aromatic C (110-160 ppm) and carbonyl C (160-220 ppm) according to Kögel-Kanbner (1997). The

194 relative concentrations of the different functional groups were calculated as the percentage of their

195 peak areas to the total aeras using MestReNova 14.0 software (Mestrelab Research, 2019, Spain).

196 Indices used to evaluate SOC recalcitrance include: alkyl C/O-alkyl C, aromaticity, aromatic C/O-

197 alkyl C, aliphatic C/aromatic C and aliphaticity (Baldock et al., 1997; Du et al., 2017). Aromaticity

198 = aromatic C / (alkyl C + O-alkyl C + aromatic C); Aliphatic C = alkyl C + O-alkyl C; Aliphaticity

199 = (alkyl C + O-alkyl C) / (alkyl C + O-alkyl C + aromatic C). The alkyl C/O-alkyl C ratio reflects

200 the degree of microbial transformation, with higher values indicating advanced decomposition and

201 accumulation of recalcitrant alkyl compounds (Baldock et al., 1997). The aromatic C/O-alkyl C

202 ration aligns with the alkyl C/O-alkyl C ration in reflecting the degree of SOC decomposition,

203 whereas the aliphatic C/aromatic C ratio presents a contrary perspective to them. Aromaticity is a

chemical concept denoting the resistance to microbial degradation (Kögel-Knabner, 1997). Aliphaticity is used to quantify the proportion of labile aliphatic components relative to stable aromatic moieties.

2.6. Thermogravimetry analysis

TG analysis was performed using a Netzsch TG 209F1 (Netzsch-Gerätebau GmbH, Selb, Germany). Air-dried soil samples were first sieved through a 2-mm mesh, and then ground in a ball mill to pass through a 50 μm sieve. The grounded soil samples (5 ~ 10 mg) were placed in an Al_2O_3 crucible covered with an aluminum lid and were oxidized in an atmosphere of 20 mL min^{-1} of synthetic air (20% O_2 and 80% N_2) and 20 mL min^{-1} of N_2 as a protective gas. The temperature program included a heating rate of 10°C min^{-1} from 40°C up to 800°C. The sample mass percentage relative to the initial mass as a function of temperature was recorded simultaneously, and its first derivative (DTG) was calculated to represent the mass loss rate.

Three processes were detected in the temperature range of 40°C to 800°C: hygroscopic moisture evaporation, SOM decomposition and carbonate breaking down (Gao et al., 2015; Siewert, 2004). Based on the observed DTG curve, the weight loss between 180°C and 530°C, representing the temperature range during which SOM was decomposed, was defined as the total mass of SOM (Exo_{tot}). The mass loss between 180°C and 380°C was a consequence of thermally labile SOM oxidation (Exo_1) and that between 380°C and 530°C was caused by the combustion of more stable organic matter (Exo_2) (Gao et al., 2015; Volkov et al., 2020). We used two parameters, the ratio of Exo_1 and Exo_{tot} (Exo_1/ Exo_{tot}) and the temperature at which half of the SOM was decomposed (TG-T_{50}), to characterize the thermal stability of SOM. Higher Exo_1/ Exo_{tot} and lower TG-T_{50} values indicate that the sample has more thermally labile or unstable SOM (Gao et al., 2015; Siewert, 2004).

2.7. Statistical analysis

Statistical analyses were carried out with R Studio software (R Development Core Team, version 4.1.2). One-way analysis of variance (ANOVA) was conducted to assess the effect of amendments on soil physico-chemical properties, SOC physical fractions, chemical composition and thermal indices. The independence of samples, normality of residuals and homogeneity of variances were checked by Chisq, Shapiro-Wilk and Bartlett test, respectively. Fisher's least significant difference (LSD) method was used for the multiple comparisons of means with a 0.05 significance level. Linear

233 regression analysis was conducted to investigate the correlations between SOC and iron oxides, soil

234 aggregation, and the relationships between pH and iron oxides. Principal component analysis (PCA)

235 was performed to evaluate the relationship between the quantity and quality of SOC and factors

236 related to chemical protection and physical protection. Pearson correlation analyses were performed

237 to explore the relationships between chemical composition and thermal indices.

238 **3. Results**

239 *3.1. Long-term pig manure application increased SOC, TN, pH, non-crystalline (Fe_o) and*

240 *improved soil aggregation*

241 Long-term manure amendment altered the soil physico-chemical properties (Table 1). Relative to

242 the Control, the SOC concentration was 64.9%, 116.2% and 126.6% higher in the LM, HM and

243 HML treatments, respectively ($P<0.05$), and TN concentration was 48.0%-108.2% higher ($P < 0.05$).

244 The pH values were 0.62-2.28 units higher than that in the Control ($P<0.05$). Application of pig

245 manure had no significant effect on crystalline iron oxides (Fe_d) content ($P>0.05$), but the HM and

246 HML treatments showed significantly greater non-crystalline iron oxides (Fe_o), with an increase of

247 25.4% relative to the Control ($P<0.05$). Compared to the Control, the HM and HML treatments had

248 significantly higher macroaggregates (>0.25 mm) content by 15.8% and 16.8%, respectively, and

249 greater mean weight diameter (MWD) by 24.3% and 35.0% ($P<0.05$). In contrast, microaggregates

250 (0.05-0.25 mm) was lower under the HM and HML treatments, with reduction of 30.4% and 36.4%,

251 respectively ($P<0.05$).

252 *3.2. Long-term pig manure application affected SOM physical fractions: MAOM and POM*

253 The distribution of MAOM and POM fractions was significantly influenced by manure and lime

254 amendments ($P<0.05$, Table 2). Across all treatments, MAOM dominated the soil mass proportion

255 (72.5%–75.1%), whereas the proportion of POM was progressively higher, ranging from 16.6% in

256 the Control to 19.3%–19.4% under the HM and HML treatments.

257 Manure application improved SOC concentration in both fractions. SOC in the MAOM fraction

258 was 32.0%-66.8% greater, and that in the POM fraction was 208%-592% greater relative to the

259 Control. The contribution of MAOM to total SOC was lower in the HM and HML treatments

260 (65.5%-65.8%) than in the Control (82.4%), while the contribution of POM was nearly threefold

261 higher (increasing from 8.8% to 23.7%–26.0%). Lime addition (HML vs. HM) did not significantly

262   alter mass proportions but further enhanced POM C concentration (+15.4%) and its contribution to

263   total SOC (+9.7%).

3.3. Effect of long-term pig manure application on SOC chemical composition and recalcitrance

265   The solid-state ^{13}C NMR spectra showed different signal patterns for the different treatments (Fig.

266   1) and quantified the ratios of the different SOC functional groups shown in Table 3. Relative to the

267   Control, the HM and HML treatments had a significantly higher proportion of alkyl C by 4.6%-4.9%

268   ($P<0.05$), while the LM treatment showed no significant difference ($P>0.05$). The proportion of O-

269   alkyl C was also significantly higher under the LM, HM and HML treatments, with increases of

270   5.5%, 2.6% and 2.2%, respectively ($P<0.05$). In contrast, the proportions of aromatic C and carbonyl

271   C were lower in the manure-amended treatments, with reduction of 12.4%-13.2% and 0.9%-8.7%,

272   respectively ($P<0.05$).

273   Relative to the Control, the alkyl C/O-alkyl C ratio was significantly lower under the LM

274   treatment ($P<0.05$), whereas the HM and HML treatments had no significant effect on the ratio ($P >$

275   0.05, Table3). The aromaticity was decreased by 14.4%, 12.9% and 13.2% under LM, HM and HML

276   treatments, respectively ($P<0.05$, Table3). Similarly, the aromatic C/O-alkyl C ratio was 14.7%-

277   17.7% lower in the manured treatment ($P<0.05$, Table3). Conversely, both the aliphatic C/aromatic

278   C ratio and aliphaticity were higher in the manured treatments, with elevations of 18.1%-20.7% and

279   2.44%-3.66%, respectively ($P<0.05$, Table3).

3.4. The effect of long-term pig manure application on SOC thermal stability

281   The shapes of TG and its first derivatives (DTG) curves showed distinct weight losses rate as

282   temperature increased to above 100°C, in the order of HM>HML>LM>Control (Fig. 2). Relative to

283   the Control treatment, pig manure application significantly increased the total mass losses in the

284   range of 180°C to 530°C (Exo_{tot}) by 11.1%- 17.4% ($P < 0.05$, Table 4), and significantly increased

285   the mass losses during 180-380°C (Exo_1) and 380-530°C (Exo_2) by 14.6%-26.5% and 7.8%-13.7%,

286   respectively ($P<0.05$, Table 4). The ratio of Exo_1/Exo_{tot} was significantly elevated in the LM and

287   HM treatments ($P<0.05$), whereas the HM treatment showed no significant effect relative to the

288   Control ($P>0.05$, Table 4). HM and HML treatments significantly decreased TG-T_{50} by 10.7-12.0 ℃

289   ($P<0.05$), while LM treatments showed no significant difference compared to Control ($P>0.05$,

290   Table 4).

3.5. *Relationships between SOC and factors related to the mineral protection and physical*

291

292   ***protection of SOC***

293   Fig. 3 showed correlations between SOC and possible variables associated with the chemical

294   protection and physical protection of SOC. SOC in the bulk soil was significantly positively

295   correlated with MAOM C (R^2=0.97, Fig. 3A). MAOM C showed no relationship with Fed (R^2=0.04,

296   Fig. 3B), but it was positively correlated with Feo (R^2=0.56, Fig. 3C). A weaker correlation was

297   observed between MAOM C and the content of clay and silt (R^2 = 0.34, P=0.46, Fig. 3D). Notably,

298 Fe_o concentration was significantly and positively correlated with pH (R^2=0.59, P<0.01; Fig. 4A).

299   Conversely, the concentration of Fe_d was not correlated with pH (P>0.05; Fig. 4B).

300   SOC in the bulk soil was significantly positively correlated with POM C (R^2=0.95, Fig. 3E). POM

301   C was significantly associated with soil aggregation, evidenced by the positive correlation with

302   macroaggregates (>0.25 mm) (R^2=0.78, Fig. 3F) and MWD (R^2=0.67, Fig. 3H), whereas a negative

303   correlation was observed with microaggregates (<0.25 mm) (R^2=-0.71, Fig. 3G).

304   A PCA plot diagram (Fig. 5) revealed distinct associations between SOC quantity/quality and

305   stabilization mechanisms. SOC vector aligned positively with POM C, macroaggregates and MWD,

306   but inversely with microaggregates. Chemically, SOC covaried with MAOM C and Fe_o, yet formed

307   an obtuse angle (>90°) with Fe_d. TG-T_{50} negatively associated with the proportion of O-alkyl C and

308   aliphaticity (angles > 90º), but positively linked to aromatic C and aromaticity (angles < 90º).

309   **4. Discussion**

310   ***4.1. POM C and physical protection***

311   Long-term pig manure application caused an increase of SOC in the bulk soil relative to the

312   Control, and the increase was mainly derived from continuous manure inputs (Gong et al., 2009).

313   Although maize rhizodeposition (including root exudates and sloughed-off cells) (typically <10%

314   of net primary productivity; Pausch and Kuzyakov, 2018) contributes to SOC during the growing

315   season, its annual carbon inputs are only 0.2-0.5 Mg C ha^{-1} yr^{-1} (Dennis et al., 2010). This plant-

316   derived C input is much lower than that from manure, which ranged from 1.6 to 6.4 Mg C ha-1 yr^{-1}

317   in the LM and HM treatments, respectively. The rigorous removal of all harvest residues (stalks and

318   recoverable roots) minimized aboveground and root biomass as a source of soil carbon deposition.

319   It should be noted that some residual plant-derived materials (e.g., fine root fragments and exudates)

have contributed marginally to the SOC pool. Given the relatively small quantity of plant-derived carbon inputs, the changes in SOC observed in this study are primarily attributable to the application of pig manure. Following microbial decomposition and transformation, the applied manure-C was progressively partitioned into distinct SOC pools.

Manure-derived carbon was preferentially allocated to the POM fraction rather than the MAOM fraction. The contribution of POM C to SOC in the manure-amended treatment was nearly threefold as that in the Control (8.8% to 26.0%), while the proportion of MAOM C decreased significantly from 82.4% in the Control to 65.4%–71.0% in the manure application treatments (Table 2). The result was in line with Lan et al. (2022) and Li et al. (2018), who reported that increased manure substitution improved the POM C/MAOM C ratio, indicating manure was beneficial to the formation of POM C.

These results implied carbon inputs are preferentially stabilized as POM rather than MAOM. This finding is supported by biomarker evidence showing a great contribution of plant-derived carbon to the POM fraction (Zou et al., 2023). Consistent with this, a ^{13}C isotopic tracing study revealed that 70%-87% of residue-derived SOC was accumulated in the POM fraction at two experimental sites (Mitchell et al.,2021). The mechanism behind this preferential sequestration is the physical occlusion of fresh organic material within macroaggregates, which provides initial protection against rapid microbial decomposition. Therefore, POM C can be a good indicator of SOC dynamics under field management (Álvaro-Fuentes et al., 2021; Wu et al., 2023).

While POM C is inherently labile and susceptible to decomposition, it can be physically protected from rapid decay through occlusion within stable soil aggregates. According to the classical hierarchical aggregation model (Six et al., 2000), organic carbon acts as a primary binding agent for microaggregates (<0.25mm) to form macroaggregates (>0.25mm), with POM serving as both a structural nucleus and a transient carbon reservoir (Six et al., 2000). In this study, macroaggregates were significantly increased, and free microaggregates were significantly decreased after pig manure application (Table 1). These results implied that manure-derived carbon acted as binding agent, promoting the formation of macroaggregates from free microaggregates. This process provides physical protection for SOC, particularly that in the POM fraction, within the newly formed aggregates, particularly in the POM fraction (Peng et al., 2023). The observed positive

349 correlation between POM C and both macroaggregates and aggregate MWD (Fig.3; Fig.4) further

350 suggested the critical role of soil aggregation. However, the physical mechanisms by which POM

351 facilitates this process (e.g., microbial mediation, hydrophobic interactions, or polysaccharide

352 bridging) require further investigation. Experimental approaches such as isotopic labelling

353 combined with micro-scale imaging (e.g., electron microscopy or X-ray computed tomography) can

354 visualize the spatial distribution of POM within aggregates and quantify its role in aggregate

355 formation. Future study should pay attention to these new technologies.

356

357 *4.2. MAOM C and chemical protection*

358   MAOM retained higher SOC concentrations (4.18-7.09 g C kg^{-1} bulk soil) than the POM fraction

359 did, irrespective of treatments, though its contribution to total SOC decreased after manure

360 application (Table 2). This underscores that organo-mineral complexation, rather than physical

361 protection within aggregates, is the primary stabilization pathway in these red soils, even under

362 significant organic input. MAOM C exhibited significantly longer mean residence time (MRT)

363 compared to POM C, with reported turnover periods of 26-40 years versus 2.4-4.3 years,

364 respectively (Benbi et al., 2014; Garten and Wullschleger, 2000). This fundamental difference

365 originates from the unique stabilization mechanism of MAOM C through persistent organo-mineral

366 associations (Lavallee et al., 2019). While clay minerals are widely recognized as key MAOM

367 stabilizers (Hemingway et al., 2019; Liang et al., 2017), our study reveals a distinct iron oxide-

368 dominated mechanism in these Fe-rich red soils. The strong correlation between MAOM C and non-

369 crystalline Fe oxides (Fe$_o$, R^2=0.56; Figs. 3C, 4) highlighted the pivotal role of Fe$_o$ on SOC

370 stabilization in this red soil. This iron-mediated stabilization likely stems from the exceptionally

371 high specific surface area of Fe$_o$ (~800 m² g^{-1} in ferrihydrite; Kleber et al., 2005) and its superior

372 capacity to form stable organo-mineral complexes (Eusterhues et al., 2005; Lehmann and Kleber,

373 2015). Previous studies have demonstrated that organic amendments can enhance the content of

374 non-crystalline Fe oxides, thereby promoting Fe-C associations (Chen et al., 2022; Huang et al.,

375 2017; Wang et al., 2019). Extending these findings, our results provide new mechanistic insight by

376 demonstrating that the increase in non-crystalline Fe oxides is closely linked to manure-induced soil

377 alkalization. Specifically, the significant positive correlation between pH and Fe$_o$ indicates that the

378 increased pH after manure application (Table 1) created conditions favoring Fe_o preservation

379 (Vithana et al., 2015), with an increase of 25.4% in the content of Fe_o. The higher Fe_o content

380 provided abundant reactive surfaces for MAOM formation. The nature of this interaction likely

381 involves specific molecular-scale binding mechanisms. Recent advances in synchrotron-based

382 spectroscopy (e.g., STXM-NEXAFS) have provided direct evidence that poorly crystalline iron

383 oxides (e.g., ferrihydrite) stabilize organic carbon primarily through ligand exchange, where

384 carboxyl (-COOH) and hydroxyl (-C-OH) functional groups in organic molecules replace the

385 surface hydroxyl groups on Fe oxides (Ruiz et al., 2024). Furthermore, coprecipitation, where

386 organic matter is encapsulated within the matrix of forming Fe (oxyhydr) oxides, represents another

387 potent stabilization mechanism that can generate long-term sinks for organic carbon (Chen et al.,

388 2014). While our bulk data cannot unequivocally distinguish between these mechanisms, the

389 correlation suggests that similar processes are likely operative in our system, contributing to the

390 stability of the large MAOM C pool. This pH-Fe_o-MAOM nexus establishes a self-reinforcing

391 stabilization mechanism: manure-derived organic ligands interact with Fe_o to form stable complexes,

392 simultaneously protecting both organic carbon and Fe_o from dissolution (Kleber et al., 2021).

393   The positive correlation between Fe_o and MAOM C (Fig. 3C) suggested that non-crystalline Fe

394 oxides played a critical role in stabilizing SOC through organo-mineral interactions. However, while

395 our data support the association between Fe_o and MAOM C, the underlying mechanisms (e.g.,

396 adsorption, co-precipitation, or ligand exchange) remain speculative due to the lack of direct

397 molecular-scale evidence. Future studies employing advanced spectroscopic techniques (e.g.,

398 synchrotron-based X-ray absorption spectroscopy or Nano-SIMS) could explicitly characterize the

399 binding forms of Fe-organic complexes, thereby validating the causal relationship between Fe_o and

400 MAOM formation.

401 *4.3. Chemical composition and thermal stability*

402   Input of new organic material could alter chemical composition of SOC and lead to the change

403 of the molecule recalcitrance of SOC (Guo et al., 2019; Yan et al., 2013; Zhou et al., 2010; Zhang

404 et al., 2013). In the current study, pig manure application resulted in a higher proportion of O-alkyl

405 C but a lower proportion of aromatic C. Given pig manure was rich in cellulose and lignin

406 components, its introduction substantially increased O-alkyl C relative to the Control (Li et al.,

2015). The considerable accumulation of O-alkyl C accounted for the reduction of the relative proportion of aromatic C and the lower aromaticity.

Long-term pig manure application strengthened SOC thermal stability by improving the content of thermally stable organic matters while it decreased TG-T_{50}. The observed increase in the absolute amount of thermally stable SOC (Exo_2) can be attributed to the formation of stable organo-mineral complexes with newly formed Fe_o. As elucidated by Kleber et al. (2021), the thermal stability of organic matter is significantly enhanced upon binding to mineral surfaces. Thermal analysis suggested that manure amend significantly increased SOM content, evidenced by the increase of the mass losses during 180-530 °C (Exo_{tot}) (Table 4). The result was consistent with the change of SOC content measured by conventional method (Table 1), indicating TG technology was promising for measuring SOM content (Siewert, 2004; Tokarski et al., 2018). The decrease of TG-T_{50} reflected more easily decomposable SOC accumulated after manure application (Gao et al., 2015; Siewert, 2004). The result consisted with that in the NMR spectroscopy, where greater O-alkyl C and higher aliphaticity were found under manure treatments (Table 3). SOC with more O-alkyl C functional groups or higher aliphaticity was less likely to resist thermochemical degradation as revealed by the negative relationship between TG-T_{50} and aliphacity (Fig. 4; Fig. 5) (Hou et al., 2019; Lehman and Kleber, 2015), thus leading to a decrease of TG-T_{50}. In this study, the thermally labile organic matters accounted for over half of the total organic matters, so the decrease of TG-T_{50} after manure application was just a result of the increased thermally organic matters not the decrease of thermal stability. In contrast, thermal stability should be strengthened according to the increased thermally stable organic matters after manure application. The observed decrease TG-T_{50} and the simultaneous increase in Exo_2 are not contradictory. This apparent paradox can be explained by the dual effect of manure amendment: the input of a large quantity of labile, manure-derived organic compounds significantly increased the proportion of thermally labile C, thereby reducing the average stability of the entire SOM pool (as reflected by the decreased TG-T_{50}). Concurrently, the manure-induced biogeochemical changes (e.g., increased pH and Fe oxide transformation) promoted the formation of highly stable organo-mineral complexes. While the relative proportion of this stable C might be diluted by the new labile C, its absolute amount within the soil system increased substantially, which is captured by the increase in the absolute Exo_2 signal. Since soil structure was destroyed due to the

436 ground process of soil samples before TG analysis, the increase of the thermally stable organic

437 matters was ascribed to mineral protection, where the correlations between organic carbon and Fe

438 oxides increased the thermally resistance of OC (Ruiz et al., 2023).

5. Conclusion

440   Manure application increased SOC quantity and improved its quality in Fe-rich red soils. SOC in

441 the POM fraction exhibited the most pronounced response to manure inputs, while the majority of

442 SOC was stored in the MAOM fraction. Furthermore, SOC was stabilized by distinct yet

443 complementary mechanisms: physical protection via aggregation process, and chemical protection

444 via Fe-organic associations induced by elevated pH. In addition, manure application increased

445 thermally stable organic matters. However, to better understand inherent mechanisms, future work

446 should focus on molecular-scale characterization of Fe-organic interactions using synchrotron

447 techniques (e.g., Fe K-edge XANES/EXAFS), and in-situ visualization of POM-mediated

448 aggregation through advanced imaging tools (e.g., SEM-TEM or μ-CT) coupled with ^{13}C-labelled

449 manure to track POM dynamics within aggregates.

450

Acknowledgments

452   This work was financially supported by the NSFC-CAS Joint Fund Utilizing Large-scale

453 Scientific Facilities (No. U1832188) and Chinese Universities Scientific Fund (2023RC047). We

454 thank Yanyan Cai and Xing Xia for laboratory assistance.

455

Author contributions

457   HR conceived the experimental approach, took soil samples from the field, carried out the

458 laboratory and data analyses, wrote the first draft of the manuscript, and contributed to subsequent

459 drafts. ZLD helped analyze NMR spectrum and revise the manuscript. WDG contributed to

460 interpretating TG data and revising the manuscript. LXM conducted the experiment of NMR. XHP

461 helped design the experiment, and analyze data. YJJ contributed to the design of field experiment

462 and the process of taking soil samples. DMY contributed to the process of writing. HZ contributed

463 to funding acquisition, conceiving the experimental approach, carrying out data interpretations, and

464 the writing of all subsequent manuscript drafts.

Conflict of Interest

Hu Zhou is a member of the editorial board of SOIL.

Code/Data availability

References

Álvaro-Fuentes, J., Franco-Luesma, S., Lafuente, V., Sen, P., Usón, A., Cantero-Martínez, C., and Arrúe, J.L.: Stover management modifies soil organic carbon dynamics in the short-term under semiarid continuous maize, Soil Till. Res., 213, 105143, https://doi.org/10.1016/j.still.2021.105143, 2021.

Amelung, W., Bossio, D., de Vries, W., Kögel-Knabner, I., Lehmann, J., Amundson, R., Bol, R., Collins, C., Lal, R., Leifeld, J., Minasny, B., Pan, G., Paustian, K., Rumpel, C., Sanderman, J., van Groenigen, J.W., Mooney, S., van Wesemael, B., Wander, M., and Chabbi, A.: Towards a global-scale soil climate mitigation strategy. Nat. Commun., 11, 5427, https://doi.org/10.1038/s41467-020-18887-7, 2020.

Baldock, J.A., Oades, J.M., Nelson, P.N., Skene, T.M., Golchin, A., and Clarke, P.: Assessing the extent of decomposition of natural organic materials using solid-state ^{13}C NMR spectroscopy, Soil Res., 35, 1061–1084, https://doi.org/10.1071/S97004, 1997.

Bai, X.X., Tang, J., Wang, W., Ma, J.M., Shi, J., and Ren, W.: Organic amendment effects on cropland soil organic carbon and its implications: A global synthesis, Catena., 231, 107343, https://doi.org/10.1016/j.catena.2023.107343, 2023.

Benbi, D.K., Boparai, A.K., and Brar, K.: Decomposition of particulate organic matter is more sensitive to temperature than the mineral associated organic matter, Soil Biol. Biochem., 70, 183-192, https://doi.org/10.1016/j.soilbio.2013.12.032, 2014.

Cambardella, C.A., and Elliott, E.J.: Particulate soil organic-matter changes across a grassland cultivation sequence, Soil Sci. Soc. Am. J., 5, 777-783, https://doi.org/10.2136/sssaj1992.03615995005600030017x, 1992.

Chen, M., Zhang, S., and Liu, L.: Organic fertilization increased soil organic carbon stability and sequestration by improving aggregate stability and iron oxide transformation in saline-alkaline soil. Plant Soil 474, 233–249. https://doi.org/10.1007/s11104-022-05326-3, 2022.

Chenu, C., Angers, D.A., Barre, P., Derrien, D., Arrouays, D., and Balesdent, J.: Increasing organic stocks in agricultural soils: Knowledge gaps and potential innovations, Soil Till. Res., 188, 41-52, https://doi.org/10.1016/j.still.2018.04.011, 2019.

Cotrufo, M.F., Ranalli, M.G., Haddix, M.L., Six, J., and Lugato, E.: Soil carbon storage informed by particulate and mineral-associated organic matter, Nature Geosci., 12, 989-996, https://doi.org/10.1038/s41561-019-0484-6, 2019.

Dennis, P.G., Miller, A.J., and Hirsch, P.R.: Are root exudates more important than other sources of rhizodeposits in structuring rhizosphere bacterial communities? FEMS Microbiol Ecol., 72, 313-327, https://doi.org/10.1111/j.1574-6941.2010.00860.x, 2010.

Eusterhues, K., Rumpel, C., and Kögel-Knabner, I.: Organo-mineral association in sandy acid forest soils: importance of specific surface area, iron oxides and micropores, Eur. J Soil Sci., 56, 753-763, https://doi.org/10.1111/j.1365-2389.2005.00710.x, 2005.

Gao, Q.Q., Ma, L.X., Fang, Y.Y., Zhang, A.P., Li, G.C., Wang, J.J., Wu, D., Wu, W.L., and Du, Z.L.: Conservation tillage for 17 years alters the molecular composition of organic matter in soil profile, Sci. Total Environ.,

762, 143116, https://doi.org/10.1016/j.scitotenv.2020.143116, 2021.

Gao, W.D., Zhou, T.Z., and Ren, T.S.: Conversion from conventional to no tillage alters thermal stability of orga-n ic matter in soil aggregates, Soil Sci. Soc. Am. J., 79, 585-594, https://doi.org/10.2136/sssaj2014.08.0334. https://doi.org/10.1016/j.scitotenv.2020.143116, 2015.

Garten, C.T., and Wullschleger, S.D.: Soil carbon dynamics beneath switchgrass as indicated by stable isotope analysis, J. Environ. Qual., 29, 645-653. https://doi.org/10.2134/jeq2000.00472425002900020036x, 2000.

Gong, W., Yan, X.Y., Wang, J.Y., Hu, T.X., and Gong, Y.B.: Long-term manure and fertilizer effects on soil organic matter fractions and microbes under a wheat–maize cropping system in northern China, Geoderma, 149, 318-324, https://doi.org/10.1016/j.geoderma.2008.12.010, 2009.

Guo, Z.C., Zhang, J.B, Fan, J., Yang, X.Y., Yi, Y.L., Han, X.R., Wang, D.Z., Zhu, P., and Peng, X.H.: Does animal manure application improve soil aggregation? Insights from nine long-term fertilization experiments. Sci. Total Environ., 660, 1029-1037, https://doi.org/10.1016/j.scitotenv.2019.01.051, 2019.

Hemingway, J.D., Rothman, D.H., Grant, K.E., Rosengard, S.Z., Eglinton, T.I., Derry, L.A., and Galy, V.: Mineral protection regulates long-term preservation of natural organic carbon, Nature, 570, 2717-2726, https://doi.org/10.1038/s41586-019-1280-6, 2019.

Hou, Y.H., Chen, Y., Chen, X., He, K., and Zhu, B.: Changes in soil organic matter stability with depth in two alp-i ne ecosystems on the Tibetan Plateau, Geoderma, 351, 153-162, https://doi.org/10.1016/j.geoderma.2019.05.034, 2019.

Huang, X., Feng, C., and Zhao, G.: Carbon Sequestration Potential Promoted by Oxalate Extractable Iron Oxides t hrough Organic Fertilization. Soil Sci. Soc. Am. J. 81, 1359–1370. https://doi.org/10.2136/sssaj2017.02.0068, 2017.

Jiang, Y.J., Zhou, H., Chen, L.J., Yuan, Y., Fang, H., Luan, L., Chen, Y., Wang, X.Y., Liu, M., Li, H.X., Peng, X.H., and Sun, B.: Nematodes and microorganisms interactively stimulate soil organic carbon turnover in the macroaggregates, Front Microbiol., 9, 2803, https://doi.org/10.3389/fmicb.2018.02803, 2018.

Kleber, M., Bourg, I.C., Coward, E.K., Hamsel, C.M., Myneni, S.C.B., and Nunan. N.: Dynamic interactions at the mineral-organic matter interface, Nat. Rev. Earth Environ., 2, 402–421, https://doi.org/10.1038/s43017-021-00162-y, 2021.

Kleber, M., Mikutta, R., Torn, M.S., and Jahn,R.: Poorly crystalline mineral phases protect organic matter in acid subsoil horizons, Eur. J. Soil Sci., 717-725, https://doi.org/10.1111/j.1365-2389.2005.00706.x, 2005.

Kögel-Knabner, I.: ^{13}C and ^{15}N NMR spectroscopy as a tool in soil organic matter studies, Geoderma, 80, 243-270, https://doi.org/10.1016/S0016-7061(97)00055-4, 1997.

Lal, R.: Soil carbon sequestration impacts on global climate change and food security, Science, 304, 1623-1627, https://doi.org/10.1126/science.1097396, 2004.

Lan, Z.J., Shan, J., Huang, Y., Liu, X. M., Lv, Z.Z., Ji, J.H., Hou, H.Q., Xia, W.J., and Liu, Y.R.: Effects of long-term manure substitution regimes on soil organic carbon composition in a red paddy soil of southern China, Soil Till. Res., 221, 105395, https://doi.org/10.1016/j.still.2022.105395, 2022.

Lavallee, J.M., Soong, J.L., Cotrufo, M.F.: Conceptualizing soil organic matter into particulate and mineral-associated forms to address global change in the 21st century, Glob. Chang Biol., 26, https://doi.org/10.1111/gcb.14859, 2019.

Le, Bissonnais, Y.: Aggregate stability and assessment of soil crustability and erodibility: I. Theory and methodology, Eur. J. Soil Sci., 47,425-437, https://doi.org/10.1111/j.1365-2389.1996.tb01843.x, 1996.

Lehmann, J., Kleber, M.: The contentious nature of soil organic matter, Nature, 528, 60-68, https://doi.org/10.1038/nature16069, 2015.

Li, J., Wen, Y., Li, X., Li, Y., Yang, X., Lin, Z., Song, Z, Cooper, J., and Zhao, B.: Soil labile organic carbon fractions

and soil organic carbon stocks as affected by longterm organic and mineral fertilization regimes in the North China Plain, Soil Till. Res., 175, 281–290, https://doi.org/10.1016/j.still.2017.08.008, 2018.

Li, Z.Q., Zhao, B.Z., Wang, Q., Cao, X.Y., and Zhang, J.B.: Differences in chemical composition of soil organic carbon resulting from long-term fertilization strategies, PLoS One, 10, e0124359, https://doi.org/10.1371/journal.pone.0124359, 2015.

Lian, T.X., Wang, G.H., Yu, Z.H., Li, Y.S., Liu, X.B., and Jin, J.: Carbon input from ^{13}C-labelled soybean residues in particulate organic carbon fractions in a Mollisol. Biol. Fertil. Soils, 52, 331-339, https://doi.org/10.1007/s00374-015-1080-6, 2015.

Liang, C., Schimel, J.P., and Jastrow, J.D.: The importance of anabolism in microbial control over soil carbon storage, Nat. MicrobioL., 2, 1–6, https://doi.org/10.1038/nmicrobiol.2017.105, 2017.

Liu, S. B., Wang, J.Y., Pu, S.Y., Blagodatskaya, E., Kuzyakov, Y., and Razavi, B. S.: Impact of manure on soil biochemical properties: A global synthesis, Sci. Total Environ., 745, 141003, https://doi.org/10.1016/j.scitotenv.2020.141003, 2020.

Mitchell, E., Scheer, C., Rowlings, D., Contrufo, F., Conant, R.T., and Grace, P.: Important constraints on soil organic carbon formation efficiency in subtropical and tropical grasslands, Glob. Change Bio., 27, 5383-5391, https://doi.org/10.1111/gcb.15807, 2021.

Mustafa A., Xu, H., Shah, S.A.A., Abrar, M.M., Maitlo, A.A., Kubar, K.A., Saeed, Q., Kamran, M., Naveed, M., Wang, B.R., Sun N., and Xu, M.G.: Long-term fertilization alters chemical composition and stability of aggregate-associated organic carbon in a Chinese red soil: evidence from aggregate fraction, C mineration, and ^{13}C NMR analyses, J. Soil Sediment, 21, 2483-2496, https://doi.org/10.1007/s11368-021-02944-9, 2021.

Nichitha, C.V, Raghaven, S., Champa, B.V., Ganapathi, G., Sudarshan V., Nandita, S., Ravikumar, D., and Nagaraja, M.S.: Role of organic manures on soil carbon stocks and soil enzyme activities in intensively managemend ginger production systems. Int. J. Recycl. Org. Waste Agric., 1579, https://doi.org/10.30486/IJROWA.2023.1977064.1579, 2023.

Pausch, J., and Kuzyakov, Y.: Carbon input by roots into the soil: Quantification of rhizodeposition from root to ecosystem cell, Global Change Biol., 24, 1-12, https://doi.org/10.1111/gcb.13850, 2018.

Peng, X.Y., Huang, Y., Duan, X.W., Yang, H., and Liu J.X.: Particulate and mineral-associated organic carbon fractions reveal the roles of soil aggregates under different land-use types in a karst faulted basin of China, Catena, 220, 106721, https://doi.org/10.1016/j.catena.2022.106721, 2023.

Poeplau, C., Don, A., Six, J., Kaiser, M., Benbi, D., Chenu, C., Cotrufo, M.F., Derrien, D., Gioacchini, P., Grand, S., Gregorich, E., Griepentrog, M., Gunina, A., Haddix, M., Kuzyakov, Y., Kühnel, A., Macdonald, L.M., Soong, J., Trigalet, S., Vermeire, M.-L., Rovira, P., van Wesemael, B., Wiesmeier, M., Yeasmin, S., Yevdokimov, I., and Nieder, R.: Isolating organic carbon fractions with varying turnover rates in temperate agricultural soils – A comprehensive method comparison, Soil Biol. Biochem., 125, 10-26, https://doi.org/10.1016/j.soilbio.2018.06.025, 2018.

Ruiz, F., Rumpel, C., Dignac, M-F., Baudin, F., and Ferreira, T. O.: Combing thermal analyses and wet-chemical extractions to assess the stability of mixed-nature soil orgnaic matter, Soil Biol. Biochem., 187, 109216, https://doi.org/10.1016/j.soilbio.2023.109216, 2023.

Ruiz, F., Bernardino, A. F., Queiroz, H. M., Otero, X. L., Rumpel, C., and Ferreira, T. O.: Iron's role in soil organic carbon (de)stabilization in mangroves under land use change, Nat. Commun., 10433, https://doi.org/10.1038/s41467-024-54447-z, 2024.

Shi, R.Y., Liu, Z.D., Li, Y., Jiang, T.M., Xu, M.G., Li, J.Y., and Xu, R.K.: Mechanisms for increasing soil resistance to acidification by long-term manure application, Soil Till. Res., 185, 77-84,

https://doi.org/10.1016/j.still.2018.09.004, 2019.

Siewert, C.: Rapid screening of soil properties using thermogravimetry, Soil Sci. Soc. Am. J. 68, 1656-1661, https://doi.org/10.2136/sssaj2004.1656, 2004.

Simpson, M.J., and Simpson, A.J.: The chemical ecology of soil organic matter molecular constituents, J. Chem. Ecol., 38, 768–784, https://doi.org/10.1007/s10886-012-0122-x, 2012.

Six, J., Elliot, E.T., and Paustian, K.: Soil macroaggregate turnover and microaggregate formation: a mechanism for C sequestratioin under no-tillage agriculture, Soil Biol. Biochem., 32, 2099-2103, https://doi.org/10.1016/S0038-0717(00)00179-6, 2000.

Six, J., Conant, R.T., Paul, E.A., and Paustian, K.: Stabilization mechanisms of soil organic matter: Implications for C-saturated of soils, Plant Soil, 241, 155-176, https://doi.org/10.1023/A:1016125726789, 2002.

Soil Survey Staff.: Soil survey laboratory information manual. Soil survey investigations report No. 45, version 2.0. R. Burt (ed.). U.S. Department of Agriculture, Natural Resources Conservation Service. https://www.nrcs.usda.gov/sites/default/files/2022-10/SSIR45.pdf, 2011.

Song, X.X., Wang, P., van Z, L., Bolan, N., Wang, H.L., Li, X.M., Cheng, K., Yang, Y., Wang, M., Liu, T.X., and Li, F.B.: Towards a better understanding of the role of Fe cycling in soil for carbon stabilization and degradation, Carbon Research, 1, 5, https://doi.org/10.1007/s44246-022-00008-2, 2022.

Tokarski, D., Kučerík, J., Kalbitz, K., Demyan, M.S., Merbach, I., Barkusky, D., Ruehlmann, J., and Siewert, C.: Contribution of organic amendments to soil organic matter detected by thermogravimetry, J. Plant Nutr. Soil Sci., 181, 664-674, https://doi.org/10.1002/jpln.201700537, 2018.

Vithana, C.L., Sullivan, L.A., Burton, E.D., and Bush, R.T.: Stability of schwertmannite and jarosite in an acidic la ndscape: Prolonged field incubation, Geoderma, 239-240, 47-57, https://doi.org/10.1016/j.geoderma.2014.09.022, 2015.

Volkov, D.S., Rogova, O.B., Proskurnin, M.A., Farkhodov, Y.R., and Markeeva, L.B.: Thermal stability of organic matter of typical chernozems under different land uses, Soil Till. Res., 197, 104500, https://doi.org/10.1016/j.still.2019.104500, 2020.

Wang, S.B., Hu, K.L., Feng, P.Y., Wei, Q., and Leghari, S.J.: Determining the effects of organic manure substitution on soil pH in Chinese vegetable fields: a meta-analysis, J. Soil. Sediment, 23, 118-130, https://doi.org/10.1007/s11368-022-03330-9, 2023.

Wang, P., Wang, J., and Zhang, H.: The role of iron oxides in the preservation of soil organic matter under long-term fertilization. J. Soils Sediments 19, 588–598. https://doi.org/10.1007/s11368-018-2085-1, 2019.

Wu, J.J., Zhang, H., Pan, Y.T., Cheng, X.L., Zhang, K.R., and Liu G.H.: Particulate organic carbon is more sensitive to nitrogen addition than mineral-associated organic carbon: A meta-analysis, Soil Till. Res., 232, 105770, https://doi.org/10.1016/j.still.2023.105770, 2023.

Yan, X., Zhou, H., Zhu, Q.H., Wang, X.F., Zhang, Y.Z., Yu, X.C., and Peng, X.H.: Carbon sequestration efficiency in paddy soil and upland soil under long-term fertilization in southern China, Soil Till. Res., 130, 42-51, https://doi.org/10.1016/j.still.2013.01.013, 2013.

Zhang, J.C., Zhang, L., Wang, P., Huang, Q.W., Yu, G.H., Li, D.C., Shen, Q.R., and Ran, W.: The role of non-crystalline Fe in the increase of SOC after long-term organic manure application to the red soil of southern China, Eur. J. Soil Sci. 64, 797-804, https://doi.org/10.1111/ejss.12104, 2013.

Zhang, B.Y., Dou, S., Guo, D., and Guan, S.: Straw inputs improve soil hydrophobicity and enhance organic carbon mineralization, Agronomy, 13, 2618, https://doi.org/10.3390/agronomy13102618, 2023.

Zhou, P., Pan, G.X., Spaccini, R., and Piccolo, A.: Molecular changes in particulate organic matter (POM) in a typical Chinese paddy soil under different long-term fertilizer treatments, Eur. J. Soil Sci., 61, 231-242, https://doi.org/10.1111/j.1365-2389.2009.01223.x, 2010.

638   Zhou, H., Fang H., Zhang, Q., Wang, Q., Chen, C., Mooney, S. J., Peng X.H., and Du, Z. L.: Biochar enhances soil
639   hydraulic function but not soil aggregation in a sandy loam, Eur. J. Soil Sci., 70, 291-300,
640   https://doi.org/10.1111/ejss.12732, 2019.

641   Zou, Z.C., Ma, L.X., Wang, X., Chen, R.R., Jones, D.L., Bol, R., Wu, D., and Du, Z.L.: Decadal application of
642   mineral fertilizers alters the molecular composition and origins of organic matter in particulate and
643   mineral-associated fractions, Soil Biol. Biochem., 182, 109042,
644   https://doi.org/10.1016/j.soilbio.2023.109042, 2023.

645

646

647 **Table 1**

648 Soil organic carbon (SOC), total nitrogen (TN), the ration of SOC to TN (SOC/TN), pH, crystalline iron oxides

649 (Fe_d), non-crystalline iron oxides (Fe_o), aggregate size distribution and mean weight diameter (MWD) of water-

650 stable aggregates under no manure (Control), low manure (LM), high manure (HM) and high manure plus lime

651 (HML) treatments.

Treatments	SOC (g kg^{-1})	TN (g kg^{-1})	SOC/TN	pH	Fe_d (g kg^{-1})	Fe_o (g kg^{-1})	Aggregate size distribution (g g^{-1})			MWD (mm)
							>0.25 mm	0.05-0.25 mm	<0.05 mm	
Control	4.79c	0.67c	7.10b	4.80c	62.99a	1.81b	0.67c	0.28a	0.05a	0.98b
LM	7.91b	1.00b	7.94a	5.42c	59.98a	1.74b	0.71b	0.25a	0.04ab	1.09b
HM	10.37a	1.35a	7.69ab	6.11b	59.59a	2.25a	0.77a	0.19b	0.03b	1.22a
HML	10.86a	1.40a	7.76ab	7.08a	62.22a	2.29a	0.78a	0.18b	0.04ab	1.32a

652 Values are the means (n=3). Different lowercase letters after values in the same row indicate a significant difference

653 among four manure treatments ($P < 0.05$).

654

655 **Table 2**

656 Mass proportion, SOC concentration and contribution of the mineral-associated organic matter (MAOM) (<53 μm)

657 fraction, particulate organic matter (POM) (>53 μm) fraction under no manure (Control), low manure (LM), high

658 manure (HM) and high manure plus lime (HML) treatments.

Treatments	Mass proportion (%)		SOC concentration (g C kg^{-1} soil)		Contribution to total SOC (%)	
	MAOM	POM	MAOM	POM	MAOM	POM
Control	74.3a	16.6b	4.18c	0.44c	82.4a	8.8c
LM	75.1a	17.2ab	5.61b	1.26b	71.0b	15.9b
HM	73.9a	19.4a	6.81a	2.46a	65.8b	23.7a
HML	72.5a	19.3a	7.09a	2.84a	65.4b	26.0a

659 Values are the means (n=3). Different lowercase letters after values in the same row indicate a significant difference

660 among four manure treatments ($P < 0.05$). Calculations follow the methodology described in Section 2.4.

661

Table 3

The contents of various C functional groups in CPMAS-^{13}C-NMR spectra under no manure (Control), low manure (LM), high manure (HM) and high manure plus lime (HML) treatments. Alkyl (0-45 ppm); O-alkyl C (45-110 ppm); aromatic C (110-160 ppm) and carbonyl C (160-220 ppm).

Treatments	alkyl C (%)	O-alkyl C (%)	aromatic C (%)	carbonyl C (%)	alkyl C/ O-alkyl C	aromaticity (%)	aromatic C/O-alkyl C	aliphatic C/ aromatic C	aliphaticity (%)
Control	25.4b	44.9c	15.3a	14.4a	0.57a	17.9a	0.34a	4.58b	82.1b
LM	26.2ab	47.4a	13.3b	13.1b	0.55b	15.3b	0.28b	5.53a	84.7a
HM	26.6a	46.1b	13.4b	13.9ab	0.58a	15.6b	0.29b	5.41a	84.4a
HML	26.5a	45.9b	13.3b	14.3a	0.58a	15.6b	0.29b	5.43a	84.4a

Values are the means (n=3). Different lowercase letters after values in the same row indicate a significant difference among four manure treatments ($P < 0.05$). Aromaticity = aromatic C/ (alkyl C + O-alkyl C + aromatic C); aliphatic C = (alkyl C + O-alkyl C); aliphaticity = (alkyl C + O-alkyl C) / (alkyl C + O-alkyl C + aromatic C).

Table 4

The mass losses during specific temperature ranges under no manure (Control), low manure (LM), high manure (HM) and high manure plus lime (HML) treatments. Exo_1 represents thermally labile soil organic matter (SOM); Exo_2 represents thermally stable SOM; Exo_{tot} represents total SOM. TG-T_{50} indicates the temperature at which half of the total SOM is lost.

Treatments	Exo_1 (180~380°C) (%)	Exo_2 (380~530°C) (%)	Exo_{tot} (180~530°C) (%)	Exo_1/Exo_{tot}	TG-T_{50} (°C)
Control	2.28c	2.36b	4.64b	0.49b	381a
LM	2.62b	2.54a	5.16a	0.51a	376ab
HM	2.69ab	2.68a	5.37a	0.50b	369b
HML	2.89a	2.56a	5.45a	0.53a	371b

Values are the means (n=3). Different lowercase letters after values in the same row indicate a significant difference among four manure treatments ($P < 0.05$).

Figure legends

687   **Fig. 1** CPMAS-^{13}C-NMR spectra under no manure (Control), low manure (LM), high manure (HM) and high

688   manure plus lime (HML) treatments. Alkyl (0-45 ppm); O-alkyl C (45-110 ppm); aromatic C (110-160 ppm) and

689   carbonyl C (160-220 ppm)

690

691   **Fig. 2** Thermogravimetry (TG) curves (a) and corresponding derivative thermogravimetry (DTG) curves (b) of soil

692   organic matter (SOM) under no manure (Control), low manure (LM), high manure (HM) and high manure plus

693   lime (HML) treatments

694

695   **Fig. 3** The relationships between SOC and variables related to the chemical protection and physical protection

696

697   **Fig. 4** Relationship between soil pH and iron oxides concentrations.

698

699   **Fig. 5** Biplots of the principal component analysis (PCA) between the quantity and quality of SOC and variables

700   related to chemical protection, physical protection across four manure application treatments (CK, Control; LM,

701   low manure; HM, high manure; and HML, high manure plus lime)

702

703   **Fig. 6** The relationships between SOC quantity, chemical recalcitrance and thermal stability

704

705

706

707 **Fig.1** CPMAS-^{13}C-NMR spectra under no manure (Control), low manure (LM), high manure (HM) and high

708 manure plus lime (HML) treatments. Alkyl (0-45 ppm); O-alkyl C (45-110 ppm); aromatic C (110-160 ppm) and

709 carbonyl C (160-220 ppm). The spectra are normalized to the total integral area of the control spectrum to

710 highlight differences in the relative abundances of carbon functional groups.

711
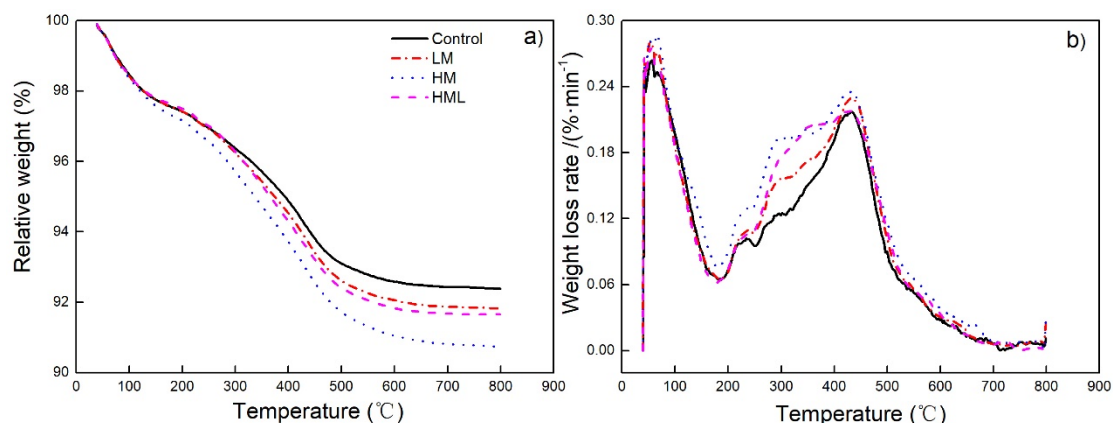
712

Fig. 2 Thermogravimetry (TG) curves (a) and corresponding derivative thermogravimetry (DTG) curves (b) of soil

organic matter (SOM) under no manure (Control), low manure (LM), high manure (HM) and high manure plus

lime (HML) treatments

716
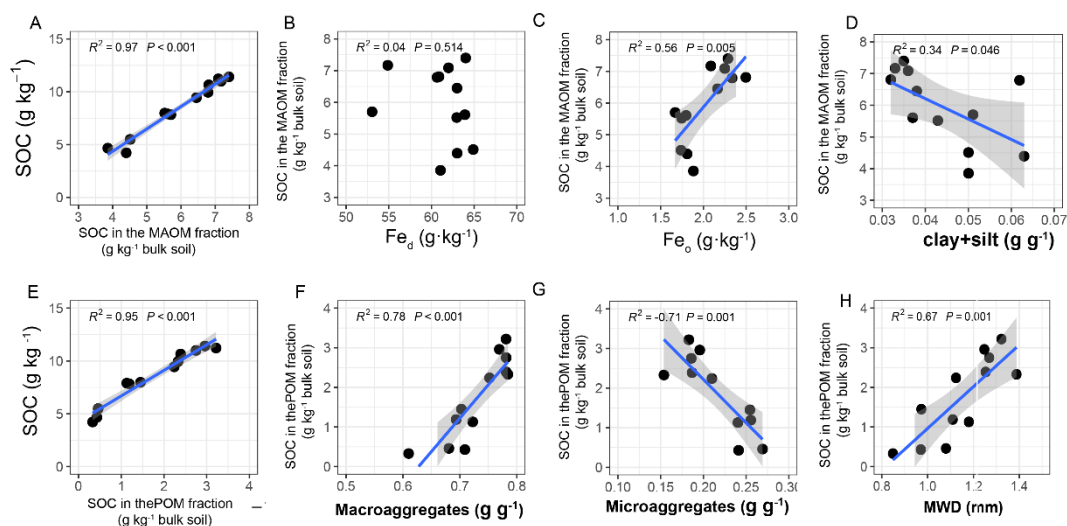
Fig. 3 The relationships between SOC and variables related to the chemical protection and physical protection. (A

to D) Variables characterizing chemical protection, including the content of SOC stored in the MAOM fraction, the

content of crystalline Fe oxides (Fe$_d$), the content of non-crystalline Fe oxides (Fe$_o$), and the content of clay and

silt. (E to H) Variables characterizing physical protection, including the content of SOC stored in the POM

fractions, the content of soil macroaggregates, the content of soil microaggregates and the mean weight diameter

(MWD)

725
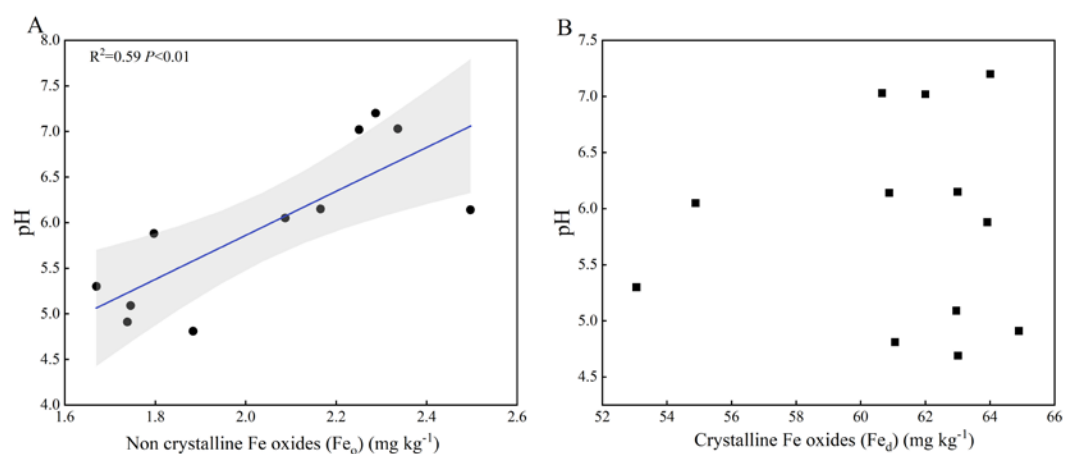
726   **Fig. 4** Relationship between soil pH and iron oxides concentrations. (A) Significant positive correlation between

727   pH and amorphous iron oxides (Fe_o). (B) No significant correlation between pH and crystalline iron oxides (Fe_d).
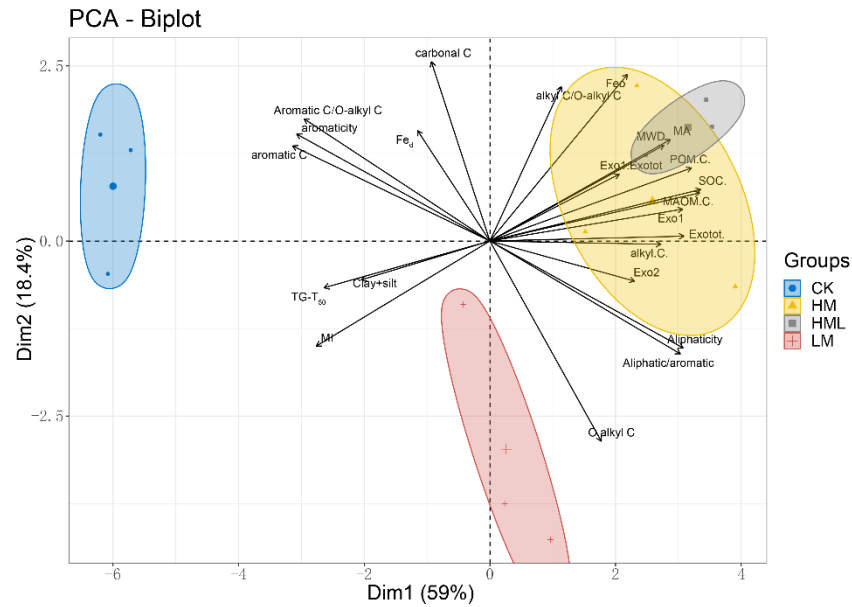
728

Fig. 5 Biplots of the principal component analysis (PCA) between the quantity and quality of SOC and variables related to chemical protection, physical protection across four manure application treatments (CK, Control; LM, low manure; HM, high manure; and HML, high manure plus lime). Fe_d, crystalline Fe oxides; Fe_o, non-crystalline Fe oxides; MA, macroaggregates (>0.25 mm); MI, microaggregates (0.05-0.25 mm); MWD, mean weight diameter; aromaticity, aromatic C / (alkyl C + O-alkyl C + aromatic C); aliphatic C, Alkyl C + O-alkyl C; aliphaticity, (Alkyl C + O-alkyl C) / (Alkyl C + O-alkyl C + Aromatic C); Exo_1, thermally labile soil organic matter (SOM); Exo_2, thermally stable SOM; Exo_{tot}, total SOM; $TG\text{-}T_{50}$, the temperature at which half of the total SOM was lost
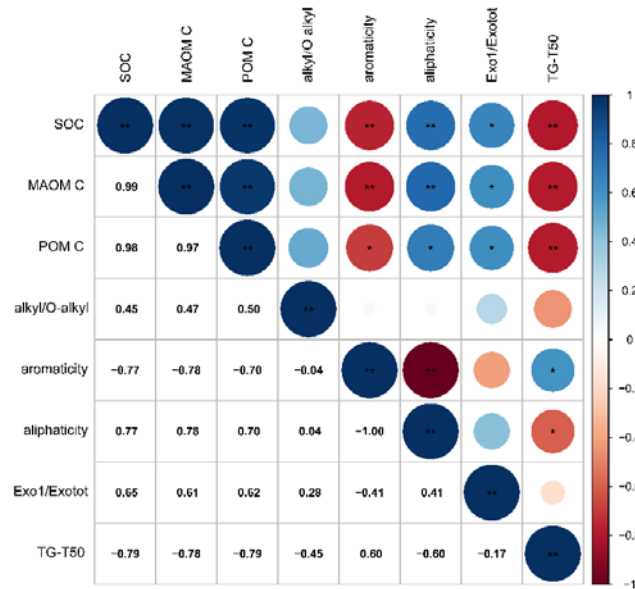
738

739 **Fig. 6** The relationships between SOC quantity, chemical recalcitrance and thermal stability. Aromaticity, aromatic

740 C / (alkyl C + O-alkyl C + aromatic C); aliphaticity, (alkyl C + O-alkyl C) / (alkyl C + O-alkyl C + aromatic C);

741 Exo_1, thermally labile soil organic matter (SOM); Exo_{tot}, total SOM; TG-T_{50}, the temperature at which half of the

742 total SOM was lost